International Journal of Radiation Oncology biology • physics

www.redjournal.org

Clinical Investigation

Impact of Pelvic Radiation Therapy for Prostate Cancer on Global Metabolic Profiles and Microbiota-Driven Gastrointestinal Late Side Effects: A Longitudinal Observational Study

Miguel R. Ferreira, PhD,[*,†,‡,§] Caroline J. Sands, PhD,[||] Jia V. Li, PhD,[¶] Jervoise N. Andreyev, PhD,[#] Elena Chekmeneva, PhD,[||] Sarah Gulliford, PhD,[*,] Julian Marchesi, PhD,[¶,††] Matthew R. Lewis, PhD,[||] and David P. Dearnaley, FRCR[*,†]**

[*]*Academic Radiotherapy Department, The Institute of Cancer Research, London, United Kingdom;* [†]*Clinical Oncology Department, The Royal Marsden NHS Foundation Trust, London, United Kingdom;* [‡]*Clinical Oncology Department, Guys and St Thomas NHS Foundation Trust, London, United Kingdom;* [§]*School of Cancer and Pharmaceutical Sciences, King's College London, London, United Kingdom;* [||]*National Phenome Centre, Faculty of Medicine, Imperial College London, London, United Kingdom;* [¶]*Department of Metabolism, Digestion and Reproduction, Imperial College, London, United Kingdom;* [#]*Gastroenterology Department, United Lincolnshire Hospitals NHS Trust, Lincolnshire, United Kingdom;* [**]*Radiotherapy Department, University College London Hospitals NHS Foundation Trust, London, United Kingdom; and* [††]*School of Biosciences, Cardiff University, Cardiff, United Kingdom*

Received Mar 29, 2021; Accepted for publication Jul 26, 2021

Abstract

Purpose: Radiation therapy to the prostate and pelvic lymph nodes (PLNRT) is part of the curative treatment of high-risk prostate cancer. Yet, the broader influence of radiation therapy on patient physiology is poorly understood. We conducted comprehensive global metabolomic profiling of urine, plasma, and stools sampled from patients undergoing PLNRT for high-risk prostate cancer.

Corresponding author: Miguel Reis Ferreira; E-mail: Miguel.ReisFerreira@kcl.ac.uk

Miguel R. Ferreira and Caroline J. Sands made equal contributions to this study.

We acknowledge support of Cancer Research UK awarded to D. Dearnaley (C8262/A7253, C1491/A9895, C1491/A15955, SP2312/021); funding from the National Institute for Health Research (NIHR) Cancer Research Network through the NIHR Biomedical Research Centre (BRC) at the Royal Marsden NHS Foundation Trust and The Institute of Cancer Research, London awarded to D. Dearnaley and M. Reis Ferreira (A53/CCR4010). This work was supported by the Medical Research Council and National Institute for Health Research (grant number MC_PC_12025) and infrastructure support was provided by the NIHR Imperial BRC. The Division of Integrative Systems Medicine and Digestive Disease at Imperial College London (J. Marchesi) receives financial support from the NIHR Imperial BRC based at Imperial College Health care NHS Trust and Imperial College London. M. Reis Ferreira acknowledges support from the Calouste Gulbenkian Foundation, the Fundação para a Ciência e a Tecnologia and the Champalimaud Foundation (SFRH/BDINTD/51547/2011), as well as from the Radiation Research Unit at the Cancer Research UK City of London Centre Award [C7893/A28990] and from the Guys and St Thomas Charity. J. Li acknowledges Medical Research Council and European Research Commission starting grants for salary support.

Disclosures: none.

Research data are stored in an institutional repository and will be shared upon request to the corresponding author.

Supplementary material associated with this article can be found, in the online version, at doi:10.1016/j.ijrobp.2021.07.1713.

Int J Radiation Oncol Biol Phys, Vol. 111, No. 5, pp. 1204–1213, 2021

https://doi.org/10.1016/j.ijrobp.2021.07.1713

Methods and Materials: Samples were taken from 32 patients at 6 timepoints: baseline, 2 to 3 and 4 to 5 weeks of PLNRT; and 3, 6, and 12 months after PLNRT. We characterized the global metabolome of urine and plasma using ^{1}H nuclear magnetic resonance spectroscopy and ultraperformance liquid chromatography-mass spectrometry, and of stools with nuclear magnetic resonance. Linear mixed-effects modeling was used to investigate metabolic changes between timepoints for each biofluid and assay and determine metabolites of interest.

Results: Metabolites in urine, plasma and stools changed significantly after PLNRT initiation. Metabolic profiles did not return to baseline up to 1 year post-PLNRT in any biofluid. Molecules associated with cardiovascular risk were increased in plasma. Pre-PLNRT fecal butyrate levels directly associated with increasing gastrointestinal side effects, as did a sharper fall in those levels during and up to 1 year postradiation therapy, mirroring our previous results with metataxonomics.

Conclusions: We showed for the first time that an overall metabolic effect is observed in patients undergoing PLNRT up to 1 year posttreatment. These metabolic changes may effect on long-term morbidity after treatment, which warrants further investigation.

Introduction

External beam radiation therapy (EBRT) is an important management option for patients with pelvic cancers. About 15,800 men receive radiation therapy for prostate cancer every year in the United Kingdom.[1] EBRT to the prostate and pelvic lymph nodes (PLNRT) may be indicated in the curative treatment of high-risk prostate cancer (PCa).[2] PLNRT targets the prostate and seminal vesicles in addition to external and internal iliac, obturator, common iliac, and presacral groups.[3] Given the wide radiation fields used with PLNRT, organs at risk such as bowel may receive significant amounts of radiation.[4] However, it is still not known how radiation therapy influences the systemic metabolism of patients. This question is made more pertinent by improvements in radiation therapy accuracy, leading to rising interest in PLNRT including large international randomized controlled trials.[5-8]

The cross-talk between radiation therapy and metabolism has been researched. For example, metabolic reprogramming in response to hypoxia and malnutrition is one of the hallmarks of cancer and may occur through aberrant overactivation of oncogenes or signaling pathways, which occur in PCa.[9] Hypoxia impairs tissue response to radiation. Historically this effect has been attributed to a decrease in oxygen radical formation during radiation.[10] More recent data indicate that anaerobic glycolysis, which creates the antioxidant lactate as a pathway end-product, is also involved in resistance to radiation.[11] Mitochondrial metabolism alterations also contribute.[12] How these changes effect host systemic metabolism is less clear. However, metabolic diseases such as diabetes mellitus increase the risk of radiation-induced side effects in patients treated for PCa, probably through impaired tissue repair and microvasculature dysfunction.[13,14] On the other hand, drugs with a metabolic effect such as metformin and statins may improve the efficacy of radiation therapy for PCa.[15,16] Clinical studies researching the effect of radiation therapy on global metabolic status are limited due to wide intersubject variation, making trends difficult to separate from the noise of high-throughput data.[17]

Metabolic phenotyping methods (including metabolomics and lipidomics) aim to measure the global, dynamic response of living systems to biological stimuli (eg, pelvic radiation therapy), with a particular focus on understanding systemic change through time in complex systems such as the human organism. High resolution proton nuclear magnetic resonance (NMR) spectroscopy and mass spectrometry (MS) are used to develop broad measurement profiles of the observable metabolome which can be investigated do discover metabolic associations with clinical observations and data. These technologies have been successfully used to detect differences in fecal metabolomes of patients with cervical cancer undergoing radiation therapy, where different metabolic profiles were detected before and after treatment.[18] However, metabolic biomarkers of radiation response remain elusive, especially with more easily accessible biofluids such as peripheral blood, urine and stools.[19] Also, all studies conducted to date focused on a single sample type and were limited by short-term follow-up.

To better understand the effect of radiation therapy on the organism as a whole, we conducted deep metabolomic analysis in patients undergoing EBRT to the prostate and pelvis for high-risk PCa, who were recruited in the Microbiota and Radiation therapy-Induced Gastrointestinal Side Effects (MARS) study.[20] Sequential samples were obtained before, during and up to 12 months after radiation therapy. We hypothesized that specific metabolic changes could be detected after radiation therapy initiation and that a recovery process could be observed after treatment. We used linear effect modeling to investigate the effect of radiation therapy treatment on the broad metabolome, after the time course of treatment and recovery while allowing for subject specific variability.

Methods

Patients

Thirty-two patients were recruited in the early cohort of the previously reported MARS study.[20] All patients were recruited before undergoing high-dose intensity modulated radiation therapy to the prostate and pelvic lymph nodes as

per a published protocol and followed longitudinally up to a year thereafter.[8] Clinical assessment and sampling was performed at baseline (preradiation therapy), at 2 to 3 weeks, 4 to 5 weeks, 12 weeks, 6 months, and 12 months postradiation therapy initiation. All subjects provided written informed consent before entry into the study. Eligibility criteria are summarized in supplementary methods. The study was approved by the Committee for Clinical Research at the Royal Marsden (no.: 4010) and by the London-Bromley Research Ethics Committee (no.: 13/LO/1527), and registered by the NHS Health Research Authority (ID: 130287). All study procedures were conducted in accordance to the Declaration of Helsinki.

Sampling procedures and sample processing

Samples (stools, urine, and plasma) obtained prior and during prostate and pelvis radiation therapy were taken before any bowel preparation procedure (rectal enema), to sample each individual's biological status as close to equilibrium (or steady-state) as possible. All sample classes were stabilized by deep freezing to −80°C as soon as reasonably possible for each particular sampling method used. Stool and urine samples were collected by patients in sterile containers, kept at room temperature, and delivered to the research team within 12 hours of collection. Fecal water was extracted as detailed in supplementary methods. Patients were instructed to collect a first-morning midstream urine sample. Nonfasting blood collection was undertaken in hospital by a trained phlebotomist. Plasma was obtained from blood as detailed in supplementary methods.

Methodology of ^{1}H NMR spectroscopy and Ultra-Performance Liquid Chromatography-Mass Spectrometry (UPLC-MS), NMR global profiling and metabolite quantification, and UPLC-MS global profiling is detailed in supplementary methods.

Statistical analysis

Before statistical analysis, metabolic profiles from urine and stool were adjusted using probabilistic quotient normalization to account for variable sample concentration.[21]

To investigate the effect of radiation therapy treatment and recovery on the broad metabolome, linear mixed effects (LME) modeling was used. For each feature, 2 LME models were generated using the lme4 package in R one with (1), and one without a factor for sampling time-point (2), both allowing for subject specific random effects, according to the following model formulae[22,23]:

(1) model_with_time <− log(feature) ∼ as.factor(time point) + (1|subjectID)

(2) model <− log(feature) ∼ 1 + (1|subjectID)

Models were compared using an approximate F-test based on the Kenward-Roger approach using the pbkrtest package and the resulting P values for all features in each data set false discovery rate (FDR) corrected using the Benjamini-Hochberg procedure.[24,25] Features with an FDR corrected P value < .05 were considered to be significantly different between sampling time points. For features of interest, post hoc contrasts were calculated using the emmeans package to further investigate metabolic changes between pairwise time points of interest (consecutively from start to end, and each time point with baseline).[26] Annotation of significant features was carried out by tandem mass spectrometry (MS/MS) for liquid chromatography-mass spectrometry (LC-MS) features and comparison of the experimental (LC-MS/MS and 1D NMR) data to in-house, online, and spectral databases in-silico.

To evaluate gastrointestinal symptoms and their relationship to metabolite levels, we closely followed our previously published methodology.[20] Patient-reported outcomes (PRO) were analyzed with the bowel subset of a gastrointestinal symptom score validated for radiation enteropathy.[27] Patients were divided in 3 groups, which were (1) no symptoms (no symptoms at either 4 or 5 weeks or 6 months); (2) nonpersistent symptoms (symptoms at either 4 or 5 weeks or 6 months); and (3) Persistent symptoms (symptoms at 4 or 5 weeks and 6 months). This strategy enables identification of patients experiencing nonhealing acute toxicity, which may be related to a consequential reaction and determines a higher risk of long-term symptoms.[28] We used LME modeling to investigate potential associations between short chain fatty acid (SCFA) metabolites of interest (butyrate and propionate) according to the model formula:

model <- log(metabolite) ∼ time point*PRO + (time point|subject)

Significance was evaluated by t tests using Satterthwaite's method.

Results

Demographics

Thirty-two men with high-risk prostate cancer were enrolled between March 18, 2014 and February 1, 2016 (Table 1). All patients underwent prostate and pelvic radiation therapy after a previously published protocol and were recruited before radiation therapy commencement, but after androgen deprivation therapy (ADT) initiation.[29] All patients were under ADT for the duration of the study and sampling period. Of the 32 men enrolled, 12 month samples were only available for 11 due to loss to follow-up.

Metabolic profiles show sample type-specific effects in the acute and late phases

LME modeling revealed significant changes in metabolic profiles between several sampling time-points (Table 2),

Table 1 Study demographics

Item	
Median age at date of enrolment in years (IQR)	66 (63-72)
Patients treated with conventionally-fractionated radiotherapy (CFRT)*; n (%)	31 (97%)
Patients treated with hypofractionated radiotherapy (HFRT)*: n (%)	1 (3%)
Median presenting PSA (IQR) in ng/mL	26.2 (13.4-47)
Gleason 6, n (%)	1 (3%)
Gleason 7, n (%)	12 (37%)
Gleason 8, n (%)	3 (9%)
Gleason 9, n (%)	16 (50%)
N0, n (%)	16 (50%)
N1, n (%)	16 (50%)
T1, n (%)	1 (3%)
T2, n (%)	7 (22%)
T3, n (%)	24 (75%)
T4, n (%)	0 (0%)
Subjects on short-course anti-androgen and long-term LHRH analogues	22 (69%)
Subjects on bicalutamide monotherapy	1 (3%)
Subjects on maximum androgen blockade	9 (28%)
Subjects on ADT at time of sampling, n (%)*	32 (100%)†
Subjects with history of abdominal or pelvic surgery, n (%)	19 (59%)
Median body mass index (IQR)	27 (25-32)
Subjects with dyslipidemia and on statins, n (%)	10 (31%)
Subjects with history of diabetes, n (%)	7 (22%)
Subjects with history of hypertension and on medical treatment, n (%)	13 (41%)
Non-smokers/ex-smokers/ smokers, n (%)	19 (59%)/11 (34%)/2 (6%)

Abbreviations: ADT = androgen deprivation therapy; IQR = interquartile range; PSA = prostate specific antigen.

* CFRT: 70 to 74 Gy to prostate and seminal vesicles (35-37 fractions) or 64 Gy to prostate bed (32 fractions); 50 to 60 Gy to pelvic lymph nodes (35-37 fractions). HFRT: 60 Gy to prostate and seminal vesicles or 55 Gy to prostate bed (20 fractions); 47 Gy to pelvic lymph nodes). †: All patients were on ADT at all sampling timepoints.

which appeared largely consistent across data sets and indeed between biofluids. Differences in metabolic profiles were observed at radiation therapy initiation (between baseline and 2 to 3 weeks of PLNRT) across all 3 biofluids. In plasma and stool samples, metabolic profiles appeared largely stable until radiation therapy completion (between 4 to 5 weeks of PLNRT and 12 weeks), and fluctuations were observed for some urine metabolites even during radiation therapy treatment. After completion of radiation therapy treatment plasma profiles again appeared to stabilize, this was not the case for urine or stool, where metabolic flux in some metabolites continued until study end. Pairwise comparisons between baseline and all other time-points showed differences in the levels of some metabolites in all 3 biofluids (although particularly in plasma and urine), indicating that metabolic differences from baseline do persist beyond the acute postradiation therapy stages.

Different metabolites change over time in different biofluids during and after radiation therapy

The results presented above showed that global metabolic profiles undergo different patterns of change in response to radiation therapy. We thus asked which metabolites showed statistically significant dynamic changes in different biofluid types. Results are summarized in Fig. 1 and in Table E1.

In plasma, we observed significant and persistent increases in triglycerides together with significant patterns in phospholipid metabolites. A significant increase in lysophosphatidylcholine was mirrored by a decrease in phosphatidylcholines, indicating increased activity of phospholipase A or lecithin-cholesterol acyltransferase.[30] Both lysophosphatidylethanolamine and phosphatidylethanolamine, which belong to a group generally termed cephalins and are associated with increased cardiovascular risk, showed a significant increase during radiation therapy.[31] Ceramides are a group of molecules implicated in processes such as apoptosis and intercell signalling. Lactosylceramides, which control processes such as cell proliferation, adhesion, migration and angiogenesis, decreased during radiation therapy.[32] Hexosylceramides, which are cerebrosides and important components of cell membranes, also decreased significantly. Plasma levels of hexosylceramides negatively associate with insulin resistance.[33] Three plasma acylcarnitines (CAR (12:0), CAR (14:1) and CAR (26:0)) decreased slowly but steadily during and after radiation therapy and were lower after treatment completion compared with baseline. Acylcarnitines are metabolites of fatty acids esterified to carnitine, which enables their transport across the mitochondrial membrane for β-oxidation. Their decrease indicates suppression of mitochondrial β-oxidation.[34] Succinate, a tricarboxylic acid (TCA) cycle intermediate and initial substrate of the oxidative phosphorylation pathway, decreased over time significantly, indicating a decrease in TCA cycle activity and energy harnessing from carbohydrate metabolism, more typical of hypoxic status. β-hydroxyisobutyrate, the major ketone body of the organism, produced within the mitochondria, mainly in the liver, decreased after treatment compared with baseline, indicating less availability of glucose or a prooxidative status, consistent with recovery postradiation therapy.[35] Citrulline, an end-product of small bowel glutamine metabolism which has been used as a marker for evaluating functional small bowel enterocyte mass and studied as a marker of radiation-

Table 2 LME modelling results between sampling time points across all datasets and biofluids

Biofluid	Assay	Assay Tailored for	Total Number of Significant Features	Baseline vs 2/3 wk of PLNRT	2/3 vs. 4/5 wk of PLNRT	4/5 wk PLNRT vs 12 wk	12 wk vs 6 mo	6 m vs 12 mo*	Baseline vs 4/5 wk of PLNRT	Baseline vs 12 wk	Baseline vs 6 mo	Baseline vs 12 mo*
Plasma	LC-MS HILIC+	Hydrophilic analytes	49	15	2	35	0	7	6	39	45	40
	LC-MS lipid RPC-	Lipophilic analytes	405	254	90	314	13	38	325	147	120	125
	LC-MS lipid RPC+	Lipophilic analytes	350	235	33	155	16	51	238	239	224	190
	NMR standard 1D	Broad compositional profile	14	5	2	9	0	4	7	10	11	13
	NMR CPMG	Small molecule analytes	6	4	1	1	0	1	5	5	6	6
	All (Number)	-	824	513	128	514	29	101	581	440	406	374
	All (Percentage)	-	(100)	**62.3**	15.5	**62.4**	3.5	12.3	**70.5**	**53.4**	**49.3**	**45.4**
Stool	NMR standard 1D	Broad compositional profile	7	5	1	3	5	3	4	1	6	1
	NMR CPMG	Small molecule analytes	65	59	2	18	22	7	50	10	13	6
	All (Number)	-	72	64	3	21	27	10	54	11	19	7
	All (Percentage)	-	(100)	**88.9**	4.17	29.2	**35.5**	13.9	**75.0**	15.28	26.4	9.7
Urine	LC-MS HILIC+	Hydrophilic analytes	0	0	0	0	0	0	0	0	0	0
	LC-MS SmMol RPC-	Small molecule analytes	16	13	4	4	4	2	9	9	7	6
	LC-MS SmMol RPC+	Small molecule analytes	7	2	2	5	1	1	2	6	3	1
	NMR standard 1D	Broad compositional profile	3	1	2	1	1	1	1	2	1	1
	All (Number)	-	26	16	8	10	6	4	12	17	11	8
	All (Percentage)	-	(100)	**61.5**	30.8	**38.5**	23.1	15.4	**46.2**	**65.4**	**42.3**	30.8

Abbreviations: CPMG: carr−purcell−meiboom−gill; HILIC: hydrophilic interaction chromatography; LC-MS: liquid chromatography-mas spectrometry; NMR: nuclear magnetic resonance; RPC: reversed phase chromatography; SmMol: small molecules.

The total number of significant features for each assay was determined by FDR correction of P values from comparison (F-test) of LME models with and without time point as a factor. Subsequent columns detail the number of those features with $P < .05$ in post-hoc pairwise comparisons (contrasts) between specified time points. Results are summarized per biofluid both in terms of total numbers and as a percentage of the total number of significant features. Pairwise time-point comparisons in which greater than a third of the total significant metabolites were observed to differ are highlighted in bold. Note, 12 months samples* were only available for 11 of the 32 patients and numbers should be interpreted with this in mind.

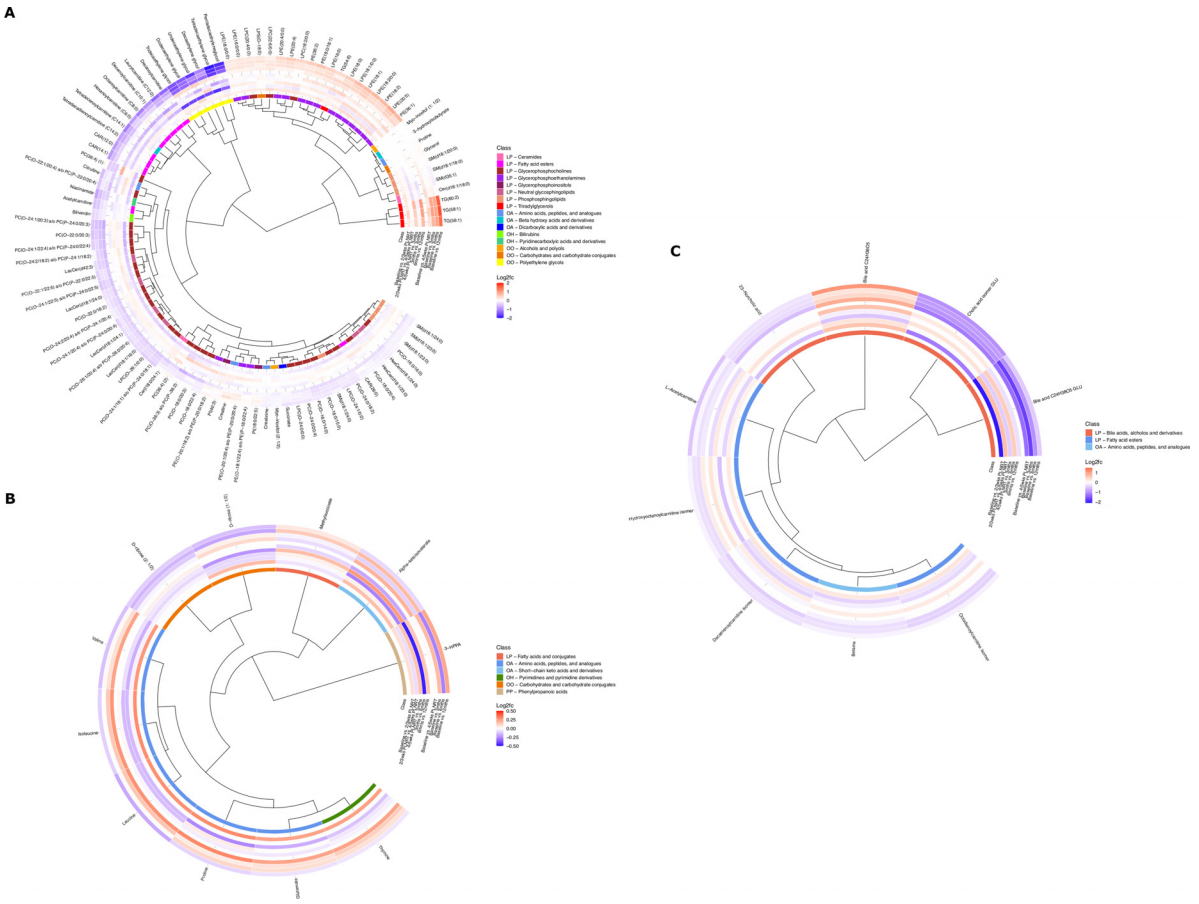

Fig. 1. Statistically significant metabolites between sampling time points in plasma (A), stool (B), and urine (C). Metabolite associations are visualized in a circular dendrogram (inner circle), surrounded by circular heatmaps for metabolic class (middle ring) and log2 fold-change values between specified sampling time-points (outer rings) for each metabolite. The magnitude of log2 fold-change is visualized using a color gradient with darker reds or blues indicating higher or lower fold-change values respectively and metabolite classes (HMDB) color-linked between panels. For log2fold-change heatmaps, the inner set of rings follow changes between consecutive time-point pairs, and the outer set display changes between each time-point and baseline. Metabolite classes comprise the following categories: LP, lipids, and lipid-like molecules; OA, organic acids and derivatives; OH, organoheterocyclic compounds; OO, organic oxygen compounds; PP, phenylpropanoids and polyketides. For full metabolite names and abbreviations see Table SI1. Multiple features annotated to the same metabolite have been combined in the figure only where the following conditions are met: (1) feature intensities across all samples correlate with Pearson correlation coefficient > 0.7; (2) contrast (*P* values) consistent, either all significant ($P < .05$) or all not-significant ($P > .05$); (3) log2 fold-change direction consistent, either all positive or all negative for significant contrast/fold-change pairs. Where multiple entries exist for the same annotation (according to these rules) annotation name is appended with the number of features combined, for example, (2 or 3) would indicate that 2 out of 3 features for this metabolite were combined in this entry.

induced small bowel toxicity, decreased at the onset of radiation therapy, although significant recovery was observed from 12 weeks postradiation therapy onwards.[36] Creatine and creatinine levels increased and decreased slightly, respectively, during and after radiation therapy, reflecting decreased creatine metabolism in muscle as a consequence of ADT.[37] Polyethylene glycols, which are common excipients in medications and are not produced endogenously, rose at radiation therapy initiation and fell back to normal after treatment completion, which is explained by uptake of supportive medications during treatment.

In urine, we noted a substantial and statistically significant decrease in excreted bile acids from the start of radiation therapy, with the exception of 7,12-dioxolithocholic acid, which significantly increased over time. Betaine, a methyl group donor and osmoprotectant with antiinflammatory properties, decreased after treatment but returned to normal at 6 months postradiation therapy.[38] In line with results in the plasma, urinary acylcarnitines decreased during and after radiation therapy.

In stools, we detected a significant increase at the start of radiation therapy in branched-chain amino acids (leucine, isoleucine, and valine). We also noted similar increases in glutamate, an acidic amino acid. Levels of these molecules normalized after radiation therapy (12 weeks). However, we observed a parallel significant increase in fecal

α-ketoisovalerate, a toxic acidogen metabolite resulting from the incomplete breakdown of BCAA, which lingered after radiation therapy completion. Levels of 3-(3-Hydroxyphenyl)propionic acid (3-HPPA), a gut microbial metabolite of dietary polyphenols reduced significantly after radiation therapy completion (ie, between 3 and 6 months), as well as when comparing baseline to 6-month levels.[39] Reduced levels of 3-HPPA can indicate alterations in the gut microbiome. Fecal ribose decreased significantly and after radiation therapy.

Short-chain fatty acid levels may stratify patients with radiation-induced GI symptoms

We previously showed that patients in this cohort with higher radiation-induced gastrointestinal symptoms have higher levels of some SCFA-producing gut bacteria, namely *Clostridium IV, Roseburia,* and *Phascolarctobacterium.*[20] We observed a trend for fecal butyrate levels falling during radiation therapy and remaining lower than baseline thereafter ($P < .01$, q = 0.06; Table E2). We therefore asked whether significant differences in fecal SCFA were detected in patients stratified by self-reported symptom levels, which we had previously found to have significantly different patterns in SCFA producers using bacterial community profiling. For this purpose, we used linear mixed models after our previously published methodology.[20] We found that butyrate rose with symptoms trending for significance (effect = 0.9; $P = .1$, Fig. 2). We noted that butyrate concentrations fell sharply in patients with symptoms, whereas they rose in patients with no symptoms, reflected in a negative effect of timepoint by symptom group (−0.16),

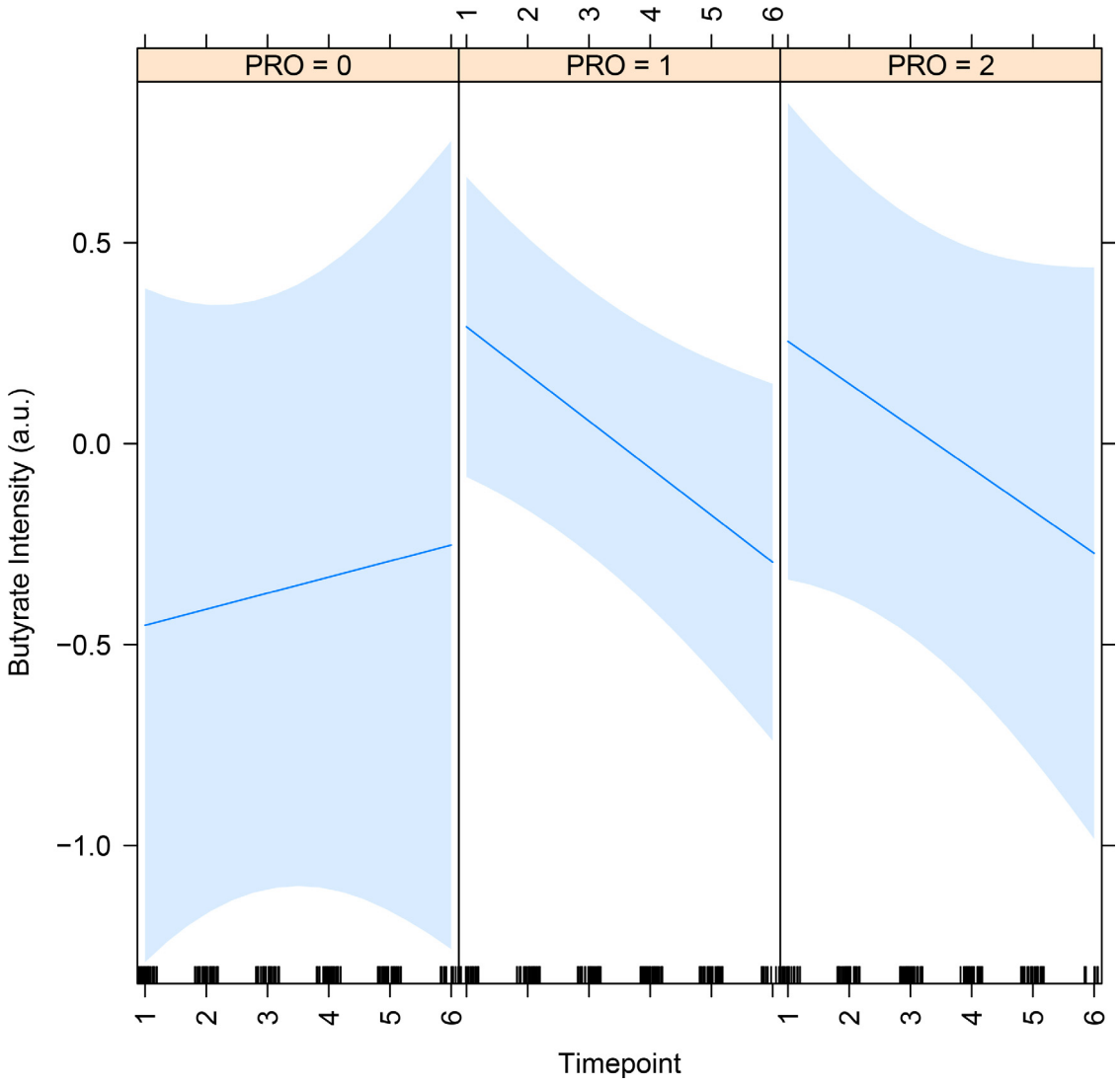

Fig. 2. Dynamic change of butyrate concentrations in stools of patients undergoing pelvic radiation therapy by patient-reported symptoms. The effect of PRO group (0.9) trended for significance ($P = .1$), meaning that the higher the symptoms, the higher the butyrate. Groups: 0 = no symptoms (n = 4), 1 = nonpersistent symptoms (n = 20), and 2 = persistent symptoms (n = 8). Timepoints: 1 = baseline, 2 = 2 or 3 weeks PLNRT, 3 = 4 or 5 weeks PLNRT, 4 = 12 weeks, 5 = 6 months, and 6 = 12 months after radiation therapy initiation. *Abbreviation*: PRO = patient-reported outcomes.

although this effect was not statistically significant ($P = .2$). We did not find significant results with propionate when stratifying patients by symptom levels.

Discussion

In this study, we showed that plasma, urine and fecal metabolomic profiles significantly changed in patients undergoing pelvic radiation therapy for high-risk prostate cancer. We also show that many of these changes relate to molecules involved in cardiovascular risk. Additionally, we demonstrate an increase in precursors of aerobic carbohydrate metabolism and increased oxidative stress. In addition, urinary bile acids decreased significantly. Fecal BCAAs and the products of their metabolism increased with radiation therapy.

In terms of coverage of the metabolome, while all methods have a finite coverage, in this analysis we employed global profiling methods which aim to be as inclusive as possible, enabling both monitoring of expected biochemicals and detection and measurement of novel, unexpected biochemicals. Ultimately, the approach doesn't preclude future discovery of other biochemicals as novel (eg, more sensitive) methods and technologies emerge, but it does provide as close to a comprehensive view of the human metabolome as is possible given modern NMR and LC-MS technologies specifically adapted for human biofluid profiling. In terms of the reproducibility of experimental methods, variation introduced by the experimental techniques including sample preparation and measurement are monitored by use of a pooled quality control sample. This allows monitoring of the data quality and removal any feature measurements not meeting commonly accepted standards in the field, details of these parameters are given in the supplementary information.[40] As with all observational findings, reproducibility in the data here is subject to follow up validation in independent cohorts.

Our study confirms previous evidence of the overall metabolic effect of radiation therapy on host metabolism.[18,19,41-43] However, to our knowledge, this is the first study in humans where patients were followed from baseline to up to a year postradiation therapy using triple biofluid sampling (urine, blood, stools). As such, it is the first study where perseverance of change is reported. We used 2 time-tested technologies to evaluate metabolomic profiles (NMR and UPLC-MS) and our statistical methodology allows for detection of group differences which are otherwise masked by intersubject variability, which is a common conundrum of "omics" studies in humans. Although the majority of assays revealed shifts in the metabolic fingerprint at largely consistent stages (ie, on radiation therapy initiation, and at some stage post radiation therapy completion) robust models were not observed between any time point pairs or in either plasma or urine for the HILIC + assay. Although it could be the case that the specific metabolites measurable by the HILIC + assay are less affected by radiation therapy treatment, it is also possible that due to some underlying structure in the data, these data sets are less successfully modelled by LME and thus retain some subject-specific variance which impedes discovery of time-specific effects.

Chai and colleagues analyzed fecal metabolomes in samples taken from 66 patients before radiation therapy (pre-RT) and before initiation of supportive therapy for GI symptoms during radiation therapy or after the last fraction of radiation therapy if no symptoms had arisen (post-RT). Eleven patients experienced GI side effects during radiation therapy.[18] Significant differences were found between pre and post-RT samples in symptomatic patients and when comparing post-RT samples between groups. Differences in pre and post-RT metabolomes of nonsymptomatic patients was not reported, which makes the data difficult to interpret and limits its clinical usefulness. Our results show that the onset of radiation therapy led to increases in valine and isoleucine (BCAAs) and decreases in glucose and butyrate over time, in agreement with the data of Chai and colleagues.[18] Of note, we detected decreased levels of butyrate in our cohort, but most particularly in patients with GI symptoms. We have previously reported no significant self-reported dietary differences between these groups of patients.[20] This observation mirrors our previously published results in the same group of patients, where we used 16S rRNA gene sequencing to profile fecal bacterial communities. We found that proportions of some bacteria producing SCFA were initially elevated but fell over time in patients with symptoms, a behavior which was mirrored when analyzing whole-microbiome SCFA-producing pathways using imputed metagenomes.[20] Metabolomic analysis also supported this observation, as butyrate concentrations also decreased significantly during treatment in patients with GI symptoms. We acknowledge that using PRO as a predictor of metabolite level is an original approach and can appear to reverse the causal relationship. However, our specific question was whether SCFA levels changed differently between patient groups stratified by symptom level over time (ie, an association rather than a causal relationship), which would require further studies including preclinical models. In addition, we mirrored our previously published methodology for the gut microbiome but this time using metabolites and as such we provide further evidence that the association between SCFA levels and radiation-induced toxicity is not trivial.[20] Chai detected decreased butyrate and acetate (another SCFA) levels in fecal samples of patients with GI symptoms.[18] Guo and colleagues recently reported that SCFA produced by the gut microbiota alleviate radiation-induced GI side effects.[44] We conclude that at least a subgroup of patients may depend on SCFA for intestinal health, as these molecules, which are produced by enteric SCFA-producing bacteria from dietary substrates, are metabolic fuels for enterocytes among other functions, including immune regulation.[45] Radiation therapy then appears to effect either the population or function of SCFA producers and other microbiota

(as highlighted by the decreasing levels of fecal 3-HPPA in our cohort), leading to decreased SCFA and, consequently, GI symptoms ensue. However, radiation enteropathy is a complex disease with disparate causes such as bile acid malabsorption, small bowel bacterial overgrowth, pancreatic insufficiency, and epithelial and endothelial damage, among other factors contributing to symptoms. The role of the microbiota in this constellation of causes remains to be fully elucidated; however, accruing evidence from several groups suggests a role of SCFA and SCFA producers in the disease pathway.[44,46] We also detected a decrease in urinary bile acid excretion, which can be associated with the phenomenon of bile acids malabsorption: one of the reported causes of radiation enteropathy.[47]

Our study shows for the first time that the onset of pelvic radiation therapy leads to increased plasma concentrations of molecules associated with cardiovascular risk through atherogenesis, increased oxidative stress and endothelial inflammatory chemokine expression, which persist after treatment completion (ie, they do not return to preradiation therapy levels), particularly triglycerides, lysophosphatidylcholines (major components of oxidised low-density lipoprotein), lysophosphatidylethanolamines, and phosphatidylethanolamines.[31] Decreases in hexosylceramide, carnitine, and in TCA cycle activity also support this observation.[48] Radiation therapy leads to increased oxidative stress, inflammation, atherosclerosis, and causes loss of vascular reactivity, cell senescence, and decreased levels of blood antioxidants, all of which may contribute to higher risk of cardiovascular events, but available evidence of clinical effect of radiation therapy without direct cardiac irradiation in heart-specific mortality and morbidity is scarce and weak.[49-51] It should also be noted that the atherogenic effects of ADT are well documented and could have contributed to the effect we observed.[52] However, patients were on ADT for a minimum of 6 months before radiation therapy onset, and the effects of ADT were settled at this point. In addition, similar changes have been previously observed in response to radiation in animal models not exposed to ADT and there was a clear effect of radiation in our cohort, making a case for higher cardiovascular risk caused by radiation therapy.[19] The possibility of increased cardiovascular risk resulting from pelvic radiation therapy should be further researched, as should its biomarkers and preventative treatments in men undergoing radiation therapy for prostate cancer. Ongoing trials of pelvic radiation therapy may be usefully explored for any such effect.

To conclude, we show that radiation therapy effects the plasma, urinary, and fecal metabolomes dynamically in patients undergoing pelvic radiation therapy. We also show that pelvic radiation therapy leads to the emergence of factors contributing to cardiovascular risk. In addition, our results with metabolic profiles are consistent with our previous metagenomic analyses, and we suggest that SCFA producers may play a significant role in radiation enteropathy. Future research should focus on identifying the clinical magnitude of these effects and the utility of trialling mitigating measures to improve the long-term survival and quality of life for men undergoing curative radiation therapy for high-risk prostate cancer.

References

1. Dearnaley D, Syndikus I, Mossop H, et al. Conventional versus hypofractionated high-dose intensity-modulated radiotherapy for prostate cancer: 5-year outcomes of the randomised, non-inferiority, phase 3 CHHiP trial. *Lancet Oncol* 2016;17:1047–1060.
2. Wilkins A, Parker C. Treating prostate cancer with radiotherapy. *Nat Rev Clin Oncol* 2010;7:583–589.
3. Harris VA, Staffurth J, Naismith O, et al. Consensus guidelines and contouring atlas for pelvic node delineation in prostate and pelvic node intensity modulated radiation therapy. *Int J Radiat Oncol Biol Phys* 2015;92:874–883.
4. Ferreira MR, Muls A, Dearnaley DP, Andreyev HJN. Microbiota and radiation-induced bowel toxicity: lessons from inflammatory bowel disease for the radiation oncologist. *Lancet Oncol* 2014;15:e139–e147.
5. Joo JH, Kim YJ, Kim YS, et al. Whole pelvic intensity-modulated radiotherapy for high-risk prostate cancer: a preliminary report. *Radiat Oncol J* 2013;31:199–205.
6. Pederson AW, Fricano J, Correa D, Pelizzari CA, Liauw SL. Late toxicity after intensity-modulated radiation therapy for localized prostate cancer: An exploration of dose−volume histogram parameters to limit genitourinary and gastrointestinal toxicity. *Int J Radiat Oncol* 2012;82:235–241.
7. McCammon R, Rusthoven KE, Kavanagh B, Newell S, Newman F, Raben D. Toxicity assessment of pelvic intensity-modulated radiotherapy with hypofractionated simultaneous integrated boost to prostate for intermediate- and high-risk prostate cancer. *Int J Radiat Oncol Biol Phys* 2009;75:413–420.
8. Reis FM, Khan A, Thomas K, et al. A phase I/II dose escalation study of the use of intensity modulated radiotherapy (IMRT) to treat the prostate and pelvic nodes in patients with prostate cancer. *Int J Radiat Oncol Biol Phys* 2017;99:1234–1242.
9. Yu Y, Gong L, Ye J. The role of aberrant metabolism in cancer: Insights into the interplay between cell metabolic reprogramming, metabolic syndrome, and cancer. *Front Oncol* 2020;10:942.
10. Wouters BG. Cell death after irradiation: How, when, and how cells die. In: Joiner MC, Van der Kogel A, eds. *Basic Clinical Radiobiology*. London, United Kingdom: Hodder Arnold; 2009:27–40.
11. Sattler UGA, Meyer SS, Quennet V, et al. Glycolytic metabolism and tumour response to fractionated irradiation. *Radiother Oncol* 2010;94:102–109.
12. Tang L, Wei F, Wu Y, et al. Role of metabolism in cancer cell radioresistance and radiosensitization methods. *J Exp Clin Cancer Res* 2018;37:87.
13. Herold DM, Hanlon AL, Hanks GE. Diabetes mellitus: A predictor for late radiation morbidity. *Int J Radiat Oncol Biol Phys* 1999;43:475–479.
14. Alashkham A, Paterson C, Hubbard S, Nabi G. What is the impact of diabetes mellitus on radiation induced acute proctitis after radical radiotherapy for adenocarcinoma prostate? A prospective longitudinal study. *Clin Transl Radiat Oncol* 2017;14:59–63.
15. Samsuri NAB, Leech M, Marignol L. Metformin and improved treatment outcomes in radiation therapy: A review. *Cancer Treat. Rev.* 2017;55:150–162.
16. Hutchinson J, Marignol L. Clinical potential of statins in prostate cancer radiation therapy. *Anticancer Res* 2017;37:5363–5372.
17. Sampson JN, Boca SM, Shu XO, et al. Metabolomics in epidemiology: Sources of variability in metabolite measurements and implications. *Cancer Epidemiol Biomarkers Prev* 2013;22:631–640.

18. Chai Y, Wang J, Wang, et al., et al. Application of 1H NMR spectroscopy-based metabonomics to feces of cervical cancer patients with radiation-induced acute intestinal symptoms. *Radiother Oncol* 2015;117:294–301.
19. Menon SS, Uppal M, Randhawa S, et al. Radiation metabolomics: Current status and future directions. *Front Oncol* 2016;6:20.
20. Reis Ferreira M, Andreyev HJN, Mohammed K. et al. Microbiota- and Radiotherapy-Induced Gastrointestinal Side-Effects (MARS) Study: A Large Pilot Study of the Microbiome in Acute and Late-Radiation Enteropathy. *Clin Cancer Res* 2019;25(21):6487–6500.
21. Dieterle F, Ross A, Schlotterbeck G, Senn H. Probabilistic Quotient normalization as robust method to account for dilution of complex biological mixtures. Application in 1H NMR metabonomics. *Anal Chem* 2006;78:4281–4290.
22. Bates D, Mächler M, Bolker BM, Walker SC. Fitting linear mixed-effects models using lme4. *J Stat Softw* 2015;67.
23. R Development Core Team, R. R: A Language and Environment for Statistical Computing. R Foundation for Statistical Computing *1*. 2011.
24. Halekoh U, Højsgaard S. A Kenward-Roger approximation and parametric bootstrap methods for tests in linear mixed models. *The R Package pbkrtest* 2014;59:1–32.
25. Benjamini Y, Hochberg Y. Controlling the false discovery rate: A practical and powerful approach to multiple testing. *J R Stat Soc Ser B* 1995;57:289–300.
26. Russell A, et al. Package 'emmeans' R topics documented. 2021;34: 216-221.
27. Olopade FA, Norman A, Blake P, et al. A modified inflammatory bowel disease questionnaire and the Vaizey incontinence questionnaire are simple ways to identify patients with significant gastrointestinal symptoms after pelvic radiotherapy. *Br J Cancer* 2005;92:1663–1670.
28. Peach MS, Showalter TN, Ohri N. Systematic review of the relationship between acute and late gastrointestinal toxicity after radiotherapy for prostate cancer. *Prostate Cancer* 2015;2015 624736.
29. Reis Ferreira M, et al. Phase 1/2 dose-escalation study of the use of intensity modulated radiation therapy to treat the prostate and pelvic nodes in patients with prostate cancer. *Int J Radiat Oncol Biol Phys* 2017;99:1234–1242.
30. Law S-H, Chan ML, Marathe GK, Parveen F, Chen CH, Ke LY. An updated review of lysophosphatidylcholine metabolism in human diseases. *Int J Mol Sci* 2019;20:1149.
31. Stegemann C, Pechlaner R, Willeit P, et al. Lipidomics profiling and risk of cardiovascular disease in the prospective population-based Bruneck study. *Circulation* 2014;129:1821–1831.
32. Chatterjee S, Pandey A. The yin and yang of lactosylceramide metabolism: Implications in cell function. *Biochim Biophys Acta* 2008;1780:370–382.
33. Chew WS, Torta F, Ji S, et al. Large-scale lipidomics identifies associations between plasma sphingolipids and T2DM incidence. *JCI Insight* 2019;5:e126925.
34. Saiki S, Hatano T, Fukamaki M, et al. Decreased long-chain acylcarnitines from insufficient β-oxidation as potential early diagnostic markers for Parkinson's disease. *Sci Rep* 2017;7:7328.
35. Chriett S, Dąbek A, Wojtala M, et al. Prominent action of butyrate over β-hydroxybutyrate as histone deacetylase inhibitor, transcriptional modulator and anti-inflammatory molecule. *Sci Rep* 2019;9:742.
36. Onal C, Kotek A, Unal B, et al. Plasma citrulline levels predict intestinal toxicity in patients treated with pelvic radiotherapy. *Acta Oncol* 2011;50:1167–1174.
37. Wyss M, Kaddurah-Daouk R. Creatine and Creatinine Metabolism. *Physiol Rev* 2000;80:1107–1213.
38. Zhao G, He F, Wu C, et al. Betaine in inflammation: Mechanistic aspects and applications. *Front Immunol* 2018;9:1070.
39. Rowland I, Gibson G, Heinken A, Scott K, Swann J, Thiele I, Tuohy K. Gut microbiota functions: Metabolism of nutrients and other food components. *Eur J Nutr* 2018;57:1–24.
40. Broadhurst D, Goodacre R, Reinke SN, et al. Guidelines and considerations for the use of system suitability and quality control samples in mass spectrometry assays applied in untargeted clinical metabolomic studies. *Metabolomics* 2018;14:72.
41. Mörén L, Wibom C, Bergström P, et al. Characterization of the serum metabolome following radiation treatment in patients with high-grade gliomas. *Radiat Oncol* 2016;11:51.
42. Jia H, Shen X, Guan Y, et al. Predicting the pathological response to neoadjuvant chemoradiation using untargeted metabolomics in locally advanced rectal cancer. *Radiother Oncol* 2018;128:548–556.
43. Ó Broin P, Vaitheesvaran B, Saha S, et al. Intestinal microbiota-derived metabolomic blood plasma markers for prior radiation injury. *Int J Radiat Oncol Biol Phys* 2015;91:360–367.
44. Guo H, Chou W, Lai Y, et al. Multi-omics analyses of radiation survivors identify radioprotective microbes and metabolites. *Science* 2020;370:eaay9097.
45. Yang W, Yu T, Huang X, et al. Intestinal microbiota-derived short-chain fatty acids regulation of immune cell IL-22 production and gut immunity. *Nat Commun* 2020;11:4457.
46. Tian T, Zhao Y-Z, Yang Y, et al. The protective role of short-chain fatty acids acting as signal molecules in chemotherapy- or radiation-induced intestinal inflammation. *Am J Cancer Res* 2020;10:3508–3531.
47. Harris V, Benton B, Sohaib A, Dearnaley D, Andreyev HJN. Bile acid malabsorption after pelvic and prostate intensity modulated radiation therapy: An uncommon but treatable condition. *J Radiat Oncol Biol Phys* 2012;84:e601–e606.
48. Wang ZY, Liu Y-Y, Liu G-H, Lu H-B, Mao C-Y. l-Carnitine and heart disease. *Life Sci* 2018;194:88–97.
49. Guo Y, Dong X, Yang F, et al. Effects of radiotherapy or radical prostatectomy on the risk of long-term heart-specific death in patients with prostate cancer. *Front Oncol* 2020;10:592746.
50. Martling A, Holm T, Johansson H, Rutqvist LE, Cedermark B. The Stockholm II trial on preoperative radiotherapy in rectal carcinoma: Long-term follow-up of a population-based study. *Cancer* 2001;92:896–902.
51. Pollack J, Holm T, Cedarmark B, et al. Late adverse effects of short-course preoperative radiotherapy in rectal cancer. *Br J Surg* 2006;93:1519–1525.
52. Lester JF, Mason MD. Cardiovascular effects of hormone therapy for prostate cancer. *Drug Heal Patient Saf* 2015;7:129–138.